Magnon dispersion in $MnWO_4$

1999 J. Phys.: Condens. Matter 11 2649

(http://iopscience.iop.org/0953-8984/11/12/019)

J. Phys.: Condens. Matter **11** (1999) 2649–2659. Printed in the UK PII: S0953-8984(99)96774-7

Magnon dispersion in $MnWO_4$

H Ehrenberg†§, H Weitzel†, H Fuess† and B Hennion‡

† Darmstadt University of Technology, D-64287 Darmstadt, Germany
‡ Laboratoire Léon Brillouin, CE Saclay, 91191 Gif Sur Yvette Cédex, France

Received 14 August 1998, in final form 14 December 1998

Abstract. The four magnon branches in the antiferromagnetic ground state of $MnWO_4$ were measured by inelastic neutron scattering for two directions. On the basis of a model including isotropic Heisenberg exchange and uniaxial anisotropy, analytical expressions were derived for the dispersion relations in the spin-wave approximation using the Holstein–Primakoff and Bogoliubov transformations. By comparison between observed and calculated excitation energies, a very reliable determination of model parameters was possible. In the framework of this model, the spin deviations at absolute zero and the propagation vector slightly below the transition temperature are calculated.

1. Introduction

In previous articles we have reported on the magnetic structures and phase transitions in $MnWO_4$ without an external field [1] and with an external magnetic field applied in different directions [2]. In zero field three antiferromagnetic phases exist. AF1 is the commensurate ground state with a collinear arrangement of eight magnetic moments in a primitive magnetic unit cell. With respect to the chemical cell the magnetic cell is described by the propagation vector $\vec{k}(\mathrm{AF1}) = \pm(-\frac{1}{4}, \frac{1}{2}, \frac{1}{2})$. The easy direction lies within the ac-plane and forms an angle of 37° with the a-axis in the $(+a, +c)$ quadrant. Depending on specific conditions, a first-order phase transition into AF2 takes place between 6.8 K and 8.0 K. The translational symmetry is described by the propagation vector $\vec{k}(\mathrm{AF2}) = (-0.2165(25), \frac{1}{2}, 0.4585(25))$, and the magnetic structure is coplanar in the plane spanned by the easy direction and [010], and ellipsoidally modulated. A second-order phase transition to AF3 occurs at $T = 12.3$ K. This phase is collinear with the same easy direction as AF1 and sinusoidally modulated according to the propagation vector $\vec{k}(\mathrm{AF3}) = (-0.2145(30), \frac{1}{2}, 0.4580(35))$, which agrees with $\vec{k}(\mathrm{AF2})$ within experimental uncertainties. The effect of an external field depends on the specific orientation: if the field is applied parallel to the easy direction of AF1 and AF3, the intermediate phase AF2 is stabilized; AF1 disappears at about $H = 2$ T and AF3 at about $H = 9$ T. A further increase in field strength induces a first-order phase transition into a high-field phase HF at about $H = 14$ T. On the other hand, an applied field parallel to [010] reduces the stability range of AF2, and AF1, AF2, and AF3 form a triple point at $T = 10$ K and $H = 10$ T. The metamorphism of these different topologies has also been studied in detail by determining the phase diagram for intermediate field directions, too. The stability ranges of all phases AF1, AF2, and AF3 are hardly affected by a field applied perpendicular to both the easy direction

§ Present address: Interdisciplinary Research Centre in Superconductivity, Madingley Road, Cambridge CB3 0HE, UK.

0953-8984/99/122649+11$19.50

and [010]. This manifold phase diagram including critical end points on one hand and the quite simple crystal structure of the wolframite type with only one magnetic site situated on a twofold rotational axis on the other make $MnWO_4$ a promising model system for the investigation of magnetic phase transitions and related critical phenomena. Reliable conclusions about the underlying magnetic interactions, however, cannot be drawn from the phase diagrams alone. For this purpose a sophisticated analysis of the magnetic excitations and their dependence on momentum transfer is essential. In this contribution we report on the determination of magnon dispersion in the ground state AF1 of $MnWO_4$ by inelastic neutron scattering for two directions of momentum transfer. The underlying couplings are deduced for a model including superexchange couplings via up to two bridging oxygen atoms and a uniaxial anisotropy by applying Holstein–Primakoff transformation in the spin-wave approximation and Bogoliubov transformation. The derived values are further used to calculate the spin deviations at $T = 0$ K and to compare the predicted propagation vector $\vec{k}$ slightly below the ordering temperature T_N with $\vec{k}$(AF3). Furthermore, the temperature dependence of the magnetic excitation energies at $\vec{q} = 0$ is given.

2. Experimental procedure

To choose an adequate instrument for this experiment the order of magnitude of the expected magnetic excitations has to be estimated first. The excitation of lowest energy $E_{min} = h\nu_{min}$, $\nu_{min} = 0.1$ THz, is known from antiferromagnetic resonance studies [3]. A rough estimation for the upper limit of the excitation spectrum $E_{max} = h\nu_{max}$, $\nu_{max} = 0.33$ THz, is derived from

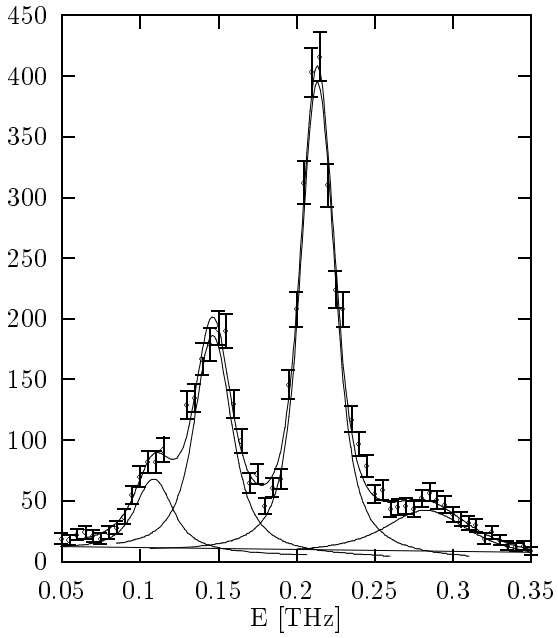

Figure 1. Observed intensities and the calculated profile for an energy scan at constant neutron momentum transfer $\vec{Q} = (\frac{1}{4}, \frac{3}{2}, -\frac{1}{2})$, i.e. magnon momentum $\vec{q} = 0$. The absolute value of the final neutron momentum was fixed at $k_f = 1.1$ Å^{-1}, and a Be filter at liquid nitrogen temperature was used to avoid $\lambda/2$ contributions.

the Néel temperature $T_N = 13.5$ K by using an empirical formula [4]. Therefore, a triple-axes spectrometer at a cold-neutron source is required for the investigation of magnon dispersion in $MnWO_4$. All experiments have been performed at the instrument 4F2 of the Laboratoire Léon Brillouin, Saclay, France, which allows for an energy resolution of about 2 GHz [5]. The appropriate scan technique for these studies was to collect intensity data at constant neutron momentum transfer $\vec{Q}$ and for different energy transfers E. The observed data have been fitted by a calculated profile, based on the response function $S(\omega)$ of a damped harmonic oscillator for the magnetic excitations [6]. Experimental data and the fitted profile are shown in figure 1 for $\vec{Q} = (\frac{1}{4}, \frac{3}{2}, -\frac{1}{2})$ as a representative transfer. The neutron momentum transfer $\vec{Q}$ is given with respect to the reciprocal lattice $\{\vec{a}^*, \vec{b}^*, \vec{c}^*\}$, defined by the standard setting of the crystal structure given in table IV of [1]. The sample was a natural single crystal from Peru with a volume of about 1 cm^3 and a mosaicity of about 1°. Small pieces from this crystal had also been used for the determination of the magnetic phase diagrams [2]. Preliminary considerations concerning the magnetic symmetries of AF1 are necessary to choose appropriate dispersion directions. With respect to the standard setting, the magnetic unit cell of AF1 is spanned by

$$\vec{a}_m = 2\vec{c} \qquad \vec{b}_m = 2\vec{b} \qquad \vec{c}_m = -2\vec{a} + \vec{c} \tag{1}$$

and the magnetic space group is $P_C 2/c$ in the notation of Opechowski and Guccione [7], which will be used further. According to the notation of Miller and Love [8] this is $A_b 2/a$, originally used for the description of this magnetic structure [9]. The parallelepiped spanned by the reciprocal-space vectors $\vec{a}_m^*$, $\vec{b}_m^*$, and $\vec{c}_m^*$ is only of half the volume of the magnetic Brillouin zone as a consequence of C symmetry. A more suitable basis for the definition of magnon momenta is therefore given by

$$\vec{g}_1 = \vec{a}_m^* + \vec{b}_m^* \qquad \vec{g}_2 = \vec{a}_m^* - \vec{b}_m^* \qquad \vec{g}_3 = -\vec{c}_m^* \tag{2}$$

and will be used from now on if not stated otherwise. Both the holosymmetric and the isogonal point groups of $P_C 2/c$ are $2/m$, and therefore the basic domain Ω and representation domain Φ are each one quarter of the magnetic Brillouin zone. Only states within the representation domain

$$\Phi = \{\vec{q} | \vec{q} = h\vec{g}_1 + k\vec{g}_2 + l\vec{g}_3;\ 0 \leqslant h \leqslant \tfrac{1}{2}, -h \leqslant k \leqslant h, -\tfrac{1}{2} \leqslant l \leqslant \tfrac{1}{2}\} \tag{3}$$

have to be considered due to Wigner's theorem. Two dispersion directions of particular interest are

$$\begin{aligned} &\text{(i) } \vec{q} = (\xi, -\xi, 0) && \xi = 0, \ldots, \tfrac{1}{2} \\ &\text{(ii) } \vec{q} = (-2\eta, -2\eta, 4\eta) && \eta = 0, \ldots, \tfrac{1}{4} \end{aligned} \tag{4}$$

because the two directions are different $\Gamma \rightarrow$ Y paths, preserving either twofold rotational symmetry (i) or mirror-plane symmetry (ii). The meaning of these directions becomes clearer if referred to the reciprocal-lattice vectors derived from the standard setting of the crystal structure, i.e. $\vec{q}' = (h', k', l') = h'\vec{a}^* + k'\vec{b}^* + l'\vec{c}^*$:

$$\begin{aligned} &\text{(i) } \vec{q}' = (0, \xi, 0) && \xi = 0, \tfrac{1}{2} \\ &\text{(ii) } \vec{q}' = (\eta, 0, -2\eta) && \eta = 0, \tfrac{1}{4}. \end{aligned} \tag{5}$$

The propagation vectors $\vec{k}$ are also given with respect to this basis. The component k_y of the propagation vector is $\frac{1}{2}$ for all phases, indicating a strong antiferromagnetic coupling parallel to [010]. Therefore, a pronounced dispersion is expected for direction (i). In the plane of special symmetry, the direction (ii) is pointed out by the ratio $k_x{:}k_z = -1{:}2$ for AF1, also nearly obeyed for AF2 and AF3. The magnon dispersion has been measured along $(\frac{1}{4}, \frac{3}{2} - \xi, -\frac{1}{2})$ and $(-\frac{1}{4}, -\frac{1}{2} + \xi, \frac{3}{2})$ for direction (i) and along $(\frac{1}{4} \pm \eta, \frac{3}{2}, -\frac{1}{2} \mp 2\eta)$ for direction (ii). The uncertainty in magnon momentum, caused by the mosaicity of the crystal, is about $\Delta\vec{q}' = (0, 0.03, 0)$ for direction (i) and $\Delta\vec{q}' = (0.01, 0.01, 0.003)$ for direction (ii).

3. The model

The primitive magnetic unit cell of the collinear ground state AF1 contains eight magnetic ions, and therefore four magnon branches are expected in zero field, each of them twofold degenerate. In this section the calculation of the dispersion relations, $\omega_{\pm}^{(j)}(\vec{q})$, $j = 1, 2$, is described. First, the model Hamiltonian is given in terms of spin-ladder operators. Then Holstein–Primakoff transformation is applied, treated in the spin-wave approximation. Finally, the Hamiltonian is diagonalized by a Bogoliubov transformation onto magnon creation and annihilation variables.

A reasonable model for the relevant magnetic interactions in $MnWO_4$ has to take into account superexchange couplings via one and two oxygens of common coordination octahedra and a uniaxial anisotropy preferring the easy direction of AF1. All experiments have been performed without an external magnetic field applied, and therefore no additional Zeeman term will be included. In a rectangular coordinate system $\{\vec{e}_\alpha, \vec{e}_\beta, \vec{e}_\gamma\}$, orientated in such a way that $\vec{e}_\gamma$ is the easy direction and $\vec{e}_\beta$ parallel to [010], the following Hamiltonian is obtained, expressed in spin-ladder operators:

$$\begin{aligned} \hat{H} &= \hat{H}_{ex} + \hat{H}_{anis} \\ \hat{H}_{ex} &= -\sum_{i \neq j} J_{ij} \left\{ \hat{S}_i^+ \hat{S}_j^- + \hat{S}_i^\gamma \hat{S}_j^\gamma \right\} \\ \hat{H}_{anis} &= -\sum_i J_{anis} \left(\hat{S}_i^\gamma\right)^2. \end{aligned} \tag{6}$$

The twofold rotational site symmetry allows for a more general anisotropy tensor, but there is no experimental evidence that more than one uniaxial parameter is required. The exchange couplings included are listed in table 1. The bond angle Mn–O–Mn in the zigzag chains is about 95°, and therefore the resulting exchange coupling J_1 is expected to be rather small [10]. This is the striking difference compared to the findings for the other 3d-transition-metal tungstates $MeWO_4$, Me = Fe, Co, and Ni, which also crystallize in the wolframite-type structure but exhibit a totally different magnetic behaviour [11].

The Hamiltonian (6) can be transformed into boson creation and annihilation operators by applying a Holstein–Primakoff transformation [12]:

$$\left.\begin{aligned} \hat{S}_j^+ &= \sqrt{2S}\varphi(n_j)a_j \\ \hat{S}_j^- &= \sqrt{2S}a_j^\dagger\varphi(n_j) \\ \hat{S}_j^\gamma &= S - a_j^\dagger a_j \end{aligned}\right\} \qquad j \in u_i;\ i = 1, \ldots, 4$$

$$\left.\begin{aligned} \hat{S}_m^+ &= \sqrt{2S}b_m^\dagger\varphi(n_m) \\ \hat{S}_m^- &= \sqrt{2S}\varphi(n_m)b_m \\ \hat{S}_m^\gamma &= -S + b_m^\dagger b_m \end{aligned}\right\} \qquad m \in u_l;\ l = 5, \ldots, 8 \tag{7}$$

with

$$\varphi(n) = \sqrt{1 - n/(2S)} \tag{8}$$

and the number operator $n = a^\dagger a$ or $b^\dagger b$, respectively, depending on the sublattice. The function φ can be expanded, and in the spin-wave approximation only terms up to first order are included and the one-particle operators are replaced by wave variables:

$$\begin{aligned} a_{u_i\vec{q}} &= \sqrt{\frac{8}{N}} \sum_{j \in u_i} \mathrm{e}^{\mathrm{i}\vec{q}\cdot\vec{r}_j} a_j \qquad i = 1, \ldots, 4 \\ b_{u_l\vec{q}} &= \sqrt{\frac{8}{N}} \sum_{m \in u_l} \mathrm{e}^{-\mathrm{i}\vec{q}\cdot\vec{r}_m} b_m \qquad l = 5, \ldots, 8 \end{aligned} \tag{9}$$

Table 1. Indirect exchange couplings for the Mn ion at $(\frac{1}{2}, y, \frac{1}{4})$ via one or two oxygens of a common octahedron, $y = 0.6853$, together with the values determined and the observed relative orientations of the two corresponding spin pairs. The anisotropy parameter is refined to $J_{anis} = 0.284\, k_B$ K.

Position of neighbour	Distance (Å)	Exchange coupling	Value (k_B K)	Spin alignment
$(\frac{1}{2}, 1-y, \frac{3}{4})$ $(\frac{1}{2}, 1-y, -\frac{1}{4})$	3.283	J_1	−0.195	↑↓, ↑↑
$(\frac{1}{2}, 2-y, \frac{3}{4})$ $(\frac{1}{2}, 2-y, -\frac{1}{4})$	4.398	J_2	−0.135	↑↓, ↑↑
$(\frac{3}{2}, y, \frac{1}{4})$ $(-\frac{1}{2}, y, \frac{1}{4})$	4.823	J_3	−0.423	↑↓, ↑↑
$(\frac{1}{2}, y, \frac{5}{4})$ $(\frac{1}{2}, y, -\frac{3}{4})$	4.992	J_4	0.414	↑↓, ↑↓
$(\frac{1}{2}, y+1, \frac{1}{4})$ $(\frac{1}{2}, y-1, \frac{1}{4})$	5.753	J_5	0.021	↑↓, ↑↓
$(\frac{3}{2}, 1-y, \frac{3}{4})$ $(-\frac{1}{2}, 1-y, -\frac{1}{4})$	5.795	J_6	−0.509	↑↓, ↑↓
$(-\frac{1}{2}, 1-y, \frac{3}{4})$ $(\frac{3}{2}, 1-y, -\frac{1}{4})$	5.873	J_7	0.023	↑↑, ↑↑
$(\frac{3}{2}, 2-y, \frac{3}{4})$ $(-\frac{1}{2}, 2-y, -\frac{1}{4})$	6.492	J_8	0.491	↑↑, ↑↑
$(-\frac{1}{2}, 2-y, \frac{3}{4})$ $(\frac{3}{2}, 2-y, -\frac{1}{4})$	6.561	J_9	−1.273	↑↓, ↑↓

and their conjugates. N is the number of magnetic ions in the crystal, and the creation and annihilation operators obey the usual commutation relations for boson operators. The dispersion relations are derived after applying the Bogoliubov transformation [13]:

$$\begin{aligned} \alpha_{i\vec{q}} &= \sum_{j=1,4} c_{ij} a_{u_i\vec{q}} + \sum_{l=5,8} c_{il} b^{\dagger}_{u_l\vec{q}} \qquad i = 1,4 \\ \beta^{\dagger}_{l\vec{q}} &= \sum_{j=1,4} c_{lj} a_{u_j\vec{q}} + \sum_{m=5,8} c_{lm} b^{\dagger}_{u_m\vec{q}} \qquad l = 5,8 \end{aligned} \tag{10}$$

with complex coefficients diagonalizing the Hamiltonian:

$$\hat{H} = \sum_{\vec{q}\in BZ} \left[\sum_{i=1,4} \omega_{i\vec{q}} \alpha^{\dagger}_{i\vec{q}} \alpha_{i\vec{q}} + \sum_{l=5,8} \omega_{l\vec{q}} \beta^{\dagger}_{l\vec{q}} \beta_{l\vec{q}} \right]. \tag{11}$$

After long but straightforward calculations [14], analytical expressions for the dispersion relations in both directions (4) are derived. They can be expressed as follows:

$$\frac{\omega^{(j)}_{\pm}(x)}{2S} = \left[c^{(j)}_0 + c^{(j)}_1 x + c^{(j)}_2 x^2 \pm \sqrt{d^{(j)}_0 + d^{(j)}_1 x + d^{(j)}_2 x^2 + d^{(j)}_3 x^3} \right]^{1/2} \qquad j = 1,2 \tag{12}$$

with

$$x = \begin{cases} \cos(2\pi\xi) & \text{for (i) } \vec{q} = (\xi, -\xi, 0) \\ \cos(4\pi\eta) & \text{for (ii) } \vec{q} = (-2\eta, -2\eta, 4\eta). \end{cases} \tag{13}$$

The coefficients are complicated expressions of second and fourth order in the model parameters, and are given in the appendix.

4. Data analysis

For a reliable determination of the model parameters it is essential to know which analytical expression and observed branch correspond to each other. This relation can only be derived from the comparison between calculated cross sections and observed intensities. Following an approach for the calculation of the cross section in the case of only two magnetic sublattices [6], the following extension to the case of eight sublattices is derived [14]:

$$\left(\frac{\mathrm{d}^2\sigma}{\mathrm{d}\Omega\,\mathrm{d}E'}\right)^{(\pm)} = \left(\frac{\mathrm{d}^2\sigma}{\mathrm{d}\Omega\,\mathrm{d}E'}\right)^{(+)} + \left(\frac{\mathrm{d}^2\sigma}{\mathrm{d}\Omega\,\mathrm{d}E'}\right)^{(-)} \tag{14}$$

with

$$\left(\frac{\mathrm{d}^2\sigma}{\mathrm{d}\Omega\,\mathrm{d}E'}\right)^{(+)} = r_0^2\frac{k_f}{k_i}F(\vec{q})^2\frac{1}{4}(1+\tilde{q}_\gamma^2)\exp\{-2W(\vec{q})\}2SN\sum_{\vec{k}\in BZ}\sum_{\vec{g}\in G}\delta(\vec{q}-\vec{k}-\vec{g})$$
$$\times\sum_{j=1}^{4}\sum_{\varphi=\alpha,\beta}(n_{\varphi_j\vec{k}}+1)\delta(\hbar\omega-\hbar\omega_{\varphi_j\vec{k}})\sum_{i,i'=1}^{8}\tilde{c}_{ij}\tilde{c}^*_{i'j}\exp\{\mathrm{i}\vec{g}\cdot\vec{\rho}_{ii'}\} \tag{15}$$

$$\left(\frac{\mathrm{d}^2\sigma}{\mathrm{d}\Omega\,\mathrm{d}E'}\right)^{(-)} = r_0^2\frac{k_f}{k_i}F(\vec{q})^2\frac{1}{4}(1+\tilde{q}_\gamma^2)\exp\{-2W(\vec{q})\}2SN\sum_{\vec{k}\in BZ}\sum_{\vec{g}\in G}\delta(\vec{q}+\vec{k}-\vec{g})$$
$$\times\sum_{j=1}^{4}\sum_{\varphi=\alpha,\beta}n_{\varphi_j\vec{k}}\delta(\hbar\omega+\hbar\omega_{\varphi_j\vec{k}})\sum_{i,i'=1}^{8}\tilde{c}^*_{ij}\tilde{c}_{i'j}\exp\{\mathrm{i}\vec{g}\cdot\vec{\rho}_{ii'}\}. \tag{16}$$

G is the reciprocal lattice spanned by (2), $\tilde{q}_\gamma$ the projection of a unit vector parallel to the momentum transfer $\vec{q}$ in the easy direction, $W(\vec{q})$ the Debye–Waller factor, r_0 the classical electron radius times the gyromagnetic ratio for a neutron, and $F(\vec{q})$ the magnetic form factor, in this application for Mn^{2+} ions. $\vec{\rho}_{ii'}$ points from any point of sublattice $u_{i'}$ to one point of u_i. The coefficients $\tilde{c}$ are defined by the back-transformation to (10):

$$\begin{aligned} a_{u_i\vec{k}} &= \sum_{j=1,4}\tilde{c}_{ij}\alpha_{j\vec{k}} + \sum_{m=5,8}\tilde{c}_{im}\beta^\dagger_{m\vec{k}} \qquad i=1,4 \\ b^\dagger_{u_l\vec{k}} &= \sum_{j=1,4}\tilde{c}_{lj}\alpha_{j\vec{k}} + \sum_{m=5,8}\tilde{c}_{lm}\beta^\dagger_{m\vec{k}} \qquad l=5,8. \end{aligned} \tag{17}$$

The extinguishing rules at the Y point are especially helpful for working out which analytical branch belongs to the observed excitations. The model parameters are then refined to give the best agreement between measured and calculated excitation energies using a least-squares algorithm; see table 1. The observed intensities have not been used for this refinement, because they provide less precise information than the observed energies. If just one parameter is varied while all others are kept fixed, changes in the third digit after the point will give a poorer agreement between observed and calculated branches; however, if all other parameters are refined again, variations in the second digit after the point will give significantly poorer agreement. Particular attention had to be given to the fact that the magnetic ground state is stable for the parameter set used, i.e. the magnetic excitation energies have to be positive definite at all points in the representation domain Φ. This is a very useful restriction of the parameter variety. Observed and calculated dispersion are compared in figure 2; the assignment of irreducible co-representations and analytical expressions to the branches is given in table 2.

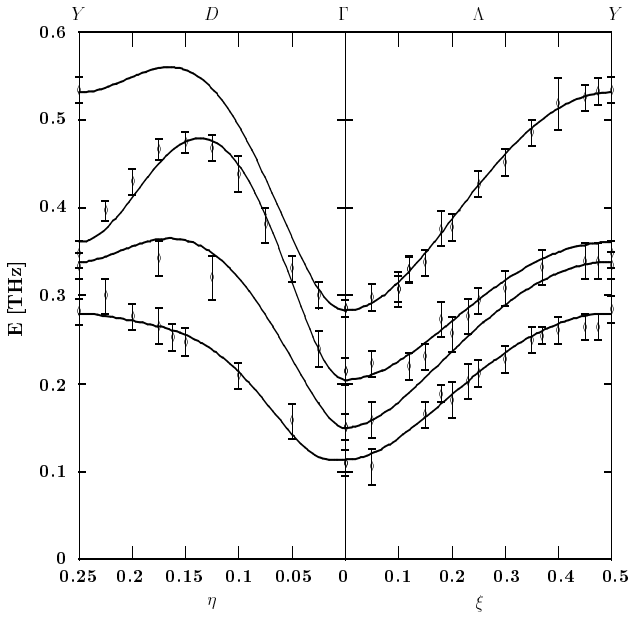

Figure 2. Observed and calculated magnetic excitation energies for magnon momenta $\vec{q}' = (-\eta, 0, 2\eta)$ and $\vec{q}' = (0, \xi, 0)$ according to (6).

This model has been confirmed by comparing the observed intensities with the cross sections, calculated according to equations (14)–(16) for the set of parameters given in table 1. No very different set of parameters can simultaneously fit the observed energies and intensities.

Table 2. Assignment of magnon symmetries and analytical expressions (12) to the observed branches, listed in order of increasing energy. All of the branches are twofold degenerate in zero field.

Γ	$\vec{q}' = (0, \xi, 0)$	Λ	$\vec{q}' = (-\eta, 0, 2\eta)$	D	Y
Γ_1^-, Γ_2^-	ω_2^-	Λ_1, Λ_2	ω_2^+	D1, D2	Y_1^-, Y_2^-
Γ_1^+, Γ_2^+	ω_2^+	Λ_1, Λ_2	ω_1^+	D1, D2	Y_1^+, Y_2^+
Γ_1^+, Γ_2^+	ω_1^-	Λ_1, Λ_2	ω_2^-	D1, D2	Y_1^+, Y_2^+
Γ_1^-, Γ_2^-	ω_1^+	Λ_1, Λ_2	ω_1^-	D1, D2	Y_1^-, Y_2^-

5. Discussion

The model presented gives a good description of the magnon dispersion in the ground state AF1 and provides reliable values for the underlying magnetic couplings. In contrast to the case for the isostructural compounds $MeWO_4$ with Me = Fe, Co, and Ni, the magnetic interactions are not dominated by a ferromagnetic 90° superexchange within the zigzag chains. For the cases with Me = Mn and Cu, the sign of the 90° superexchange is not determined by the symmetry of the Me^{2+} wave functions, and the resulting coupling is expected to be weak. This is confirmed for $MnWO_4$ by the weak superexchange coupling J_1. The strongest super-superexchange coupling J_9 is antiferromagnetic and belongs to the pair of spins at the furthest distance. This is in agreement with our findings for the case of Me = Cu, based on the excitation

energies of $CuWO_4$ [15] and the comparison of the magnetic structures of $CuWO_4$ and of the isostructural compound $CuMoO_4$-III [16]. Accordingly, the antiferromagnetic couplings are stronger for larger bond angles Cu–O–O and O–O–Cu within the exchange path Cu–O–O–Cu, and consequently the strongest coupling belongs to the furthest Cu–Cu distance, too. In the copper compounds, shorter and longer Cu–O bonds exist due to the Jahn–Teller effect, and only super-superexchange couplings via short Cu–O bonds are relatively strong [16]. In $MnWO_4$ there is no similar effect suppressing some of the possible super-superexchange path, and a system of highly competing interactions results. For example, the spin pairs coupled by J_4 are forced to an antiparallel alignment by the more dominant couplings J_6, J_8, and J_9, although a ferromagnetic arrangement would be favoured as $J_4 > 0$. For the couplings J_1, J_2, and J_3, both parallel and antiparallel spin pairs exist in AF1, and, therefore, these couplings do not contribute to the ground-state energy. Nevertheless, they are of importance for the magnetic properties at non-zero temperature and in applied magnetic fields, as reflected in the complicated magnetic phase diagram.

Based on the coupling constants derived, predictions about the magnetic properties of $MnWO_4$ can be made and compared with other experimental results. For example, the propagation vector $\vec{k}$ at a temperature slightly below the ordering temperature T_N can be deduced from the exchange couplings by maximizing an arbitrary eigenvalue of the Fourier transform of the exchange matrix with respect to k_x, k_y, and k_z. Including the couplings listed in table 1, one eigenvalue is given by

$$\begin{aligned}\lambda(k_x,k_y,k_z) = {} & J_3\cos X + J_4\cos Z + J_5\cos Y \\ & + \{[J_1\cos Z + J_6\cos(X+\tfrac{1}{2}Z) + J_7\cos(X-\tfrac{1}{2}Z)]^2 \\ & + [J_2\cos Z + J_8\cos(X+\tfrac{1}{2}Z) + J_9\cos(X-\tfrac{1}{2}Z)]^2 \\ & + 2\cos Y[J_1\cos Z + J_6\cos(X+\tfrac{1}{2}Z) + J_7\cos(X-\tfrac{1}{2}Z)] \\ & \times [J_2\cos Z + J_8\cos(X+\tfrac{1}{2}Z) + J_9\cos(X-\tfrac{1}{2}Z)]\}^{1/2} \end{aligned} \tag{18}$$

where the following abbreviations have been introduced:

$$X = 2\pi k_x \qquad Y = 2\pi k_y \qquad Z = 2\pi k_z. \tag{19}$$

For the specific values listed in table 1, the propagation vector $\vec{k} = (-0.285, \frac{1}{2}, 0.445)$ is calculated, which is in quite good agreement with the observed value, namely $\vec{k}(\mathrm{AF3}) = (-0.2145(30), \frac{1}{2}, 0.4580(35))$.

The classical Néel configuration cannot be the correct ground state AF1, because it is not even an eigenstate of the Hamiltonian (6). Nevertheless it should be a rather good approximation, and the expected deviations in the sublattice magnetizations can be estimated in the framework of the model discussed:

$$\begin{aligned}\delta S_i &= \frac{1}{N_i}\sum_{\vec{q}\in BZ}\langle a^\dagger_{\vec{q}} a_{\vec{q}}\rangle \\ &= \frac{1}{N_i}\sum_{\vec{q}\in BZ}\left[\sum_{j=1,4}\tilde{c}^*_{ij}\tilde{c}_{ij}\langle\alpha^\dagger_{j\vec{q}}\alpha_{j\vec{q}}\rangle + \sum_{m=5,8}\tilde{c}^*_{im}\tilde{c}_{im}(1+\langle\beta^\dagger_{m\vec{k}}\beta_{m\vec{k}}\rangle)\right]. \end{aligned} \tag{20}$$

This value is the same for all sublattices and can be simplified at absolute zero to

$$\delta S = \frac{1}{N_i}\sum_{\vec{q}\in BZ}\sum_{m=5,8}|\tilde{c}_{im}|^2 \tag{21}$$

for an arbitrary $i \in \{1,\ldots,4\}$, because

$$\lim_{T\to 0}\langle\alpha^\dagger_{j\vec{q}}\alpha_{j\vec{q}}\rangle = \lim_{T\to 0}\langle\beta^\dagger_{m\vec{q}}\beta_{m\vec{q}}\rangle = 0 \qquad \forall\, i,m. \tag{22}$$

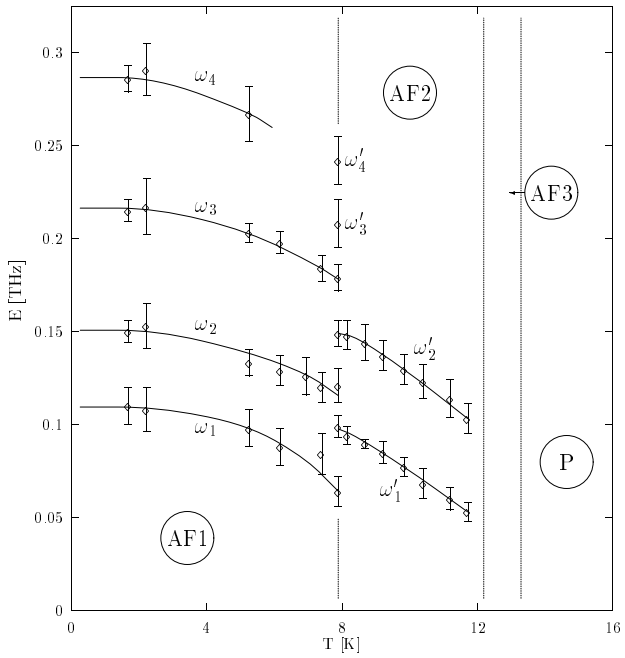

Figure 3. Temperature dependences of the magnetic excitations at the Γ point of AF1 and Γ′ of AF2 and AF3, respectively. The lines are guides for the eyes.

A numerical calculation gives $\delta S = 0.160$, in good agreement with the observed sublattice magnetization of 4.5(1) μ_B at 1.5 K and 4.6(1) μ_B at 1.2 K [1] for the $S = \frac{5}{2}$ state of Mn^{2+}.

The temperature dependence of the magnetic excitation energies is of particular interest, especially near to the transition temperatures. Although discussed only qualitatively, the softening of magnetic modes in AF1 should be stabilized discontinuously by the first-order transition to AF2, while the transition AF2 → AF3 should be accompanied by a continuous stabilization of the magnetic modes. Figure 3 displays the temperature dependence of the excitations for magnon momentum $\vec{q} = 0$, i.e. at the Γ point for AF1 and at Γ′ for AF2. At higher temperatures only a quasieleastic broadening was observed, but no individual excitations could have been resolved.

Acknowledgments

Financial support by the *Bundesminister für Bildung und Forschung* (grant Nos 03-FU3DAR and 03-WE4DAR5) and the European Community in the framework of the TMR programme is gratefully acknowledged.

Appendix

In order to obtain comprehensive expressions for the analytical dispersion relations (12) the coefficients $c_n^{(j)}$, $d_m^{(j)}$, $j = 1, 2$, $n = 0, 1, 2$, $m = 0, \ldots, 3$ have been introduced. In this appendix the specific coefficients are expressed in terms of the exchange couplings $J_1, \ldots, J_9$ and the anisotropy parameter J_{anis} for both directions under consideration. The following

abbreviation will be used:

$$J = 2(J_4 + J_5 + J_6 - J_7 - J_8 + J_9) - J_{anis}. \tag{A.1}$$

Direction (i) $\vec{q} = (-\xi, \xi, 0)$:

$$\begin{aligned}
c_0^{(1)} &= J^2 + 2JJ_3 - 4\left[J_4^2 + J_6^2 - J_7^2 - J_8^2 + J_9^2 + J_1(J_6 - J_7) + J_2(J_9 - J_8) + J_3J_4\right] \\
c_1^{(1)} &= 4\left[J_1(J_8 - J_9) + J_2(J_7 - J_6) - J_3J_5\right] + 8(J_7J_8 - J_4J_5 - J_6J_9) \\
c_2^{(1)} &= -4J_5^2
\end{aligned} \tag{A.2}$$

$$\begin{aligned}
d_0^{(1)} &= -\alpha^2 + \beta^2 + \gamma^2 \\
d_1^{(1)} &= 2(\beta\gamma + \beta\delta + \gamma\epsilon) \\
d_2^{(1)} &= \alpha^2 + \delta^2 + \epsilon^2 + 2\beta\epsilon + 2\gamma\delta \\
d_3^{(1)} &= 2\delta\epsilon
\end{aligned} \tag{A.3}$$

$$\begin{aligned}
\alpha &= 4\left[2J_7J_9 - 2J_6J_8 + J_1(J_9 - J_8) + J_2(J_7 - J_6)\right] \\
\beta &= 2J(2J_7 + J_1) - 4\left[J_3(J_6 - J_7) + J_4(2J_6 + J_1)\right] \\
\gamma &= 2J(2J_8 + J_2) + 4\left[J_3(J_8 - J_9) - J_4(2J_9 + J_2)\right] \\
\delta &= -4J_5(2J_6 + J_1) \\
\epsilon &= -4J_5(2J_9 + J_2).
\end{aligned} \tag{A.4}$$

The other set of coefficients $c_n^{(2)}, n = 0, 1, 2$, and $d_m^{(2)}, m = 0, \ldots, 3$, are also derived from (A.2)–(A.4) after replacing J_1, J_2, J_3 by $-J_1, -J_2, -J_3$.

Direction (ii) $\vec{q} = (-2\eta, -2\eta, 4\eta)$:

$$\begin{aligned}
c_0^{(1)} &= (J + 2J_8)^2 - 4(J_5 + J_6)^2 \\
c_1^{(1)} &= 4\left[J_7(J + 2J_8) - 2(J_5 + J_6)(J_4 + J_9)\right] \\
c_2^{(1)} &= 4\left[J_7^2 - (J_4 + J_9)^2\right]
\end{aligned} \tag{A.5}$$

$$\begin{aligned}
c_0^{(2)} &= (J - 2J_8)^2 - 4(J_5 - J_6)^2 \\
c_1^{(2)} &= -4\left[J_7(J - 2J_8) + 2(J_5 - J_6)(J_4 - J_9)\right] \\
c_2^{(2)} &= 4\left[J_7^2 - (J_4 - J_9)^2\right].
\end{aligned} \tag{A.6}$$

The coefficients of fourth order are also given by (A.3) but with different auxiliaries:

$$\begin{aligned}
\alpha^{(1)} &= 2(J_2 + J_3)^2 - 2J_1^2 \\
\beta^{(1)} &= 2(J_2 + J_3)(J + 2J_8) - 4J_1(J_5 + J_6) \\
\gamma^{(1)} &= 2J_1(J + 2J_8) - 4(J_3 + J_2)(J_5 + J_6) \\
\delta^{(1)} &= 4J_7(J_3 + J_2) - 4J_1(J_4 + J_9) \\
\epsilon^{(1)} &= 4J_1J_7 - 4(J_4 + J_9)(J_3 + J_2)
\end{aligned} \tag{A.7}$$

$$\begin{aligned}
\alpha^{(2)} &= 2(J_2 - J_3)^2 - 2J_1^2 \\
\beta^{(2)} &= 2(J_2 - J_3)(J - 2J_8) - 4J_1(J_5 - J_6) \\
\gamma^{(2)} &= 2J_1(J - 2J_8) + 4(J_3 - J_2)(J_5 - J_6) \\
\delta^{(2)} &= 4J_7(J_3 - J_2) - 4J_1(J_4 - J_9) \\
\epsilon^{(2)} &= 4(J_4 - J_9)(J_3 - J_2) - 4J_1J_7.
\end{aligned} \tag{A.8}$$

References

[1] Lautenschläger G, Weitzel H, Vogt T, Hock R, Böhm A, Bonnet M and Fuess H 1993 *Phys. Rev.* B **48** 6087

[2] Ehrenberg H, Weitzel H, Heid C, Fuess H, Wltschek G, Kroener T, van Tol J and Bonnet M 1997 *J. Phys.: Condens. Matter* **9** 3189

[3] Moiseev V A and Zvyagin A I 1970 *Sov. Phys.–Solid State* **12** 1454
[4] Eremenko V V and Naumenko V M 1968 *Pis. Zh. Eksp. Teor. Fiz.* **7** 416
[5] Petitgrand D 1987 *Equipements Experimentaux* 45, Laboratoire Léon Brillouin, p 45
[6] Lovesey S W 1984 *Theory of Neutron Scattering from Condensed Matter* vol 2 (Oxford: Oxford University Press)
[7] Opechowski W and Guccione R 1965 Magnetic symmetry *Magnetism* vol IIA, ed G T Rado and H Suhl (New York: Academic) ch 3, pp 105–65
[8] Miller S C and Love W F 1967 *Tables of Irreducible Representations of Space Groups and Co-Representations of Magnetic Space Groups* (Boulder, CO: Pruett)
[9] Dachs H, Stoll E and Weitzel H 1967 *Z. Kristallogr.* **125** 120
[10] Kanamori J 1959 *J. Phys. Chem. Solids* **10** 87
[11] Weitzel H and Langhof H 1977 *J. Magn. Magn. Mater.* **4** 265
[12] Holstein T and Primakoff H 1940 *Phys. Rev.* **58** 1098
[13] Bogoliubov N N 1962 *Phys. Abh. Sowjetunion* **6** 113
Bogoliubov N N 1962 *Phys. Abh. Sowjetunion* **6** 229
[14] Ehrenberg H 1996 *Thesis* Darmstadt University of Technology
[15] Lake B, Tennant D A, Cowley R A, Axe J D and Chen C K 1996 *J. Phys.: Condens. Matter* **8** 8613
[16] Ehrenberg H, Wiesmann M, Garcia-Jaca J, Weitzel H and Fuess H 1998 *J. Magn. Magn. Mater.* **182** 152